FOREX Publication
Open Access | Rapid and quality publishing

International Journal of Electrical and Electronics Research (IJEER)
Research Article | Volume 13, Issue 4 | Pages 920-931 | e-ISSN: 2347-470X

Deep Learning-Driven Expiry Date Recognition on Medicine Bottles *via* YOLOv8 Segmentation and Multi-Stage Image Denoising

Saistha N[1*], and Dr. S. Sridevi[2]
[1]*Research Scholar, Department of Computer Science and Engineering, VELS Institute of Science, Technology and Advanced Studies, Chennai, India; Email: saisthashajakan@gmail.com*
[2]*Associate Professor, Department of Computer Science and Engineering, VELS Institute of Science, Technology and Advanced Studies, Chennai, India; Email: sridevis.se@vistas.ac.in*

***Correspondence:** *Saistha N, Email: saisthashajakan@gmail.com*

ABSTRACT- Automated expiry date recognition (EDR) on pharmaceutical packaging is essential for ensuring medicine safety and minimizing waste, but it poses challenges due to text unpredictability, environmental interference, and intricate label geometries. This study presents a comprehensive deep learning system that integrates sophisticated picture pre-processing with YOLOv8-based instance segmentation to overcome these restrictions. A curated dataset including 1,000 high-resolution photos of pharmaceutical bottles, encompassing various lighting situations, camera angles, and date formats, was assembled. The pre-processing pipeline incorporates wavelet denoising, BM3D filtering, and contrast-limited adaptive histogram equalization (CLAHE) to alleviate glare and enhance low-contrast text artefacts. The advanced YOLOv8 architecture utilizes multi-scale feature fusion for accurate text localization on curved and uneven surfaces. Comparative assessments reveal the framework's superiority over leading models (Mask R-CNN, U-Net, and FCN) in segmentation precision, attaining a 95.7% F1 score and a 34% decrease in boundary error (ASD). Ablation research verifies the impact of each pre-processing step. The technology, in conjunction with an OCR module, facilitates comprehensive expiry date extraction with a character error rate (CER) of 0.9% under optimum settings. The method, although based on a restricted dataset, demonstrates significant potential for real-time quality management in pharmaceutical supply chains, enhancing AI-driven compliance monitoring and sustainable healthcare practices.

Keywords: Pharmaceutical Packaging, Expiry Date Detection, Deep Learning Segmentation, Real-Time OCR, Healthcare Automation.

ARTICLE INFORMATION
Author(s): Saistha N, Dr. S. Sridevi;
Received: 05/09/2025; **Accepted:** 09/12/2025; **Published:** 30/12/2025;
E- ISSN: 2347-470X;
Paper Id: IJEER 0509A08;
Citation: 10.37391/ijeer.130432
Webpage-link:
https://ijeer.forexjournal.co.in/archive/volume-13/ijeer-130432.html

Publisher's Note: FOREX Publication stays neutral with regard to jurisdictional claims in Published maps and institutional affiliations.

1. INTRODUCTION

Accurate expiry dates on pharmaceutical packaging are crucial for medicine safety affecting patient health and global healthcare sustainability. Misidentification of expiration labels leads to an estimated $10 billion in waste from discarded pharmaceuticals and poses serious concerns, including unfavourable patient outcomes and regulatory noncompliance. Despite breakthroughs in automated text recognition systems using DL models like CNNs and transformer architectures, detecting medication expiration dates remains a challenge. Medical packaging requires domain specific adaptation due to particular challenges such as embossed or laser etched text on curved surfaces, label glare from blister packs, and varied date formats (*e.g.*, YYYY-MM-DD, MM/YYYY) [1].

Current automated systems are effective for standardised retail environments, but fall short in pharmaceutical contexts due to three fundamental shortcomings. Domain general models do not account for medical packaging artefacts, such as low contrast lettering on translucent bottles or labels obscured by tamper-proof seals. Existing datasets do not account for real-world variability in pharmaceutical logistics, such as extreme illumination angles (ranging from 0° to 45°) and motion-blurred photos from handheld inspections. Disjointed text localisation and recognition pipelines can lead to cascade mistakes, such as misaligned segmentation masks, which can reduce downstream OCR performance by up to 40% in clinical trials [2].

Limitations prevent scalable deployment in time sensitive environments such as hospitals and supply chain hubs. This research addresses gaps in expiry date identification by taking a pharmaceutical centric approach, utilising unique dataset curation, optimised pre-processing, and an integrated

FOREX Publication
Open Access | Rapid and quality publishing
International Journal of Electrical and Electronics Research (IJEER)
Research Article | Volume 13, Issue 4 | Pages 920-931|e-ISSN: 2347-470X

DL architecture. Our medical packaging solution prioritises label geometry and regulatory text standards, improving detection accuracy and aligning with worldwide healthcare systems [2]. The important contributions of this research are summarised below

- ***Domain-Specific Dataset:*** A meticulously curated and annotated collection of 1,000 pharmaceutical label images that encapsulate real-world difficulties such as glare, low-contrast lettering, and varied date formats.
- ***Improved Pre-Processing:*** An innovative combination of wavelet denoising, BM3D filtering, and CLAHE to address text degradation on curved surfaces, with its effects measured via an ablation study.
- ***Enhanced YOLOv8 Architecture:*** Execution and verification of YOLOv8-seg for accurate expiry date segmentation, exhibiting higher efficacy compared to benchmark models.
- ***Thorough Validation:*** Stringent assessment involving 5-fold cross-validation and a comparative study with transformer-based OCR, ensuring a solid evaluation of model generalisability.
- ***End-to-End System:*** A cohesive framework encompassing picture collecting to data parsing, attaining great precision and exhibiting potential for real-time implementation.

2. LITERATURE REVIEW

Recent developments DL have greatly improved automation in several fields, especially in object detection, medical imaging, license plate recognition (LPR), and EDR. Studies such as Manlises et al. (2023) and Seker & Ahn (2022) show the effectiveness of CNNs such VGG16 and fully convolutional networks in correctly recognizing expiration dates on packaged goods, so attaining up to 97.74% accuracy using frameworks robust to diverse date formats and synthetic data augmentation in the context of food safety and waste reduction. While Salvi et al. (2020) highlight the need of pre and post processing techniques to maximize DL models in digital pathology, Li et al. (2024) and Nisa et al. (2020) underline the transforming power of CNNs and transfer learning in improving diagnostic accuracy for pathologies across organs. Using YOLO architectures and SRGAN based image augmentation, LPR systems as investigated by Khanna et al. (2025) and Ga et al. (2023) address low resolution imagery and complicated surroundings, hence attaining real-time detection with over 98% accuracy. Advancing instance segmentation for applications that range from medical cell detection to underwater debris monitoring, object detection frameworks including Mask R-CNN optimizations by Delight & Velswamy (2021) and YOLOv8-Seg enhancements by Alsuwaylimi (2024) showcase precision rates up to 94%. By means of enhanced accuracy, efficiency, and adaptability across challenging tasks, these studies collectively show the flexibility of DL in tackling real world problems, hence enabling advances in automation, sustainability, healthcare, and public safety.

Table 1. Image Recognition Literature Summary

Domain	Key Studies	Methods	Key Contributions	Performance Metrics	Applications
Expiry Date Recognition	Manlises et al. (2023) [3]	VGG16 CNN	Real-time detection of dot-matrix dates on canned goods using Raspberry Pi.	90 % accuracy (27/30 samples)	Food safety, waste reduction
	Rebedea (2020) [4]	Synthetic data + OCR	Augmented datasets improved OCR accuracy for expiry dates.	+9.4% vs. real-data models	Smart refrigerators, assistive tech
	Seker & Ahn (2022) [5]	Fully Convolutional Networks	Generalized framework for 13 date formats; released Exp. Date dataset.	97.74% recognition accuracy	Retail automation, inventory management
	Gong et al. (2021) [6]	FCN + CRNN	Dual-network system for "use by" dates under complex retail conditions.	>95% accuracy	Food quality control, compliance tracking
Medical Imaging	Li et al. (2024) [7]	CNNs, Transfer Learning	Comprehensive review of DL in organ-specific diagnostics (brain, lung, pathology).	N/A (Review)	Disease detection, image segmentation
	Nisa et al. (2020) [8]	CNNs, RNNs, Autoencoders	Automated feature extraction for improved tumor classification.	Outperformed traditional ML	Radiology, digital pathology
	Salvi et al. (2020) [9]	Pre-/Post-processing + DL	Enhanced DL robustness in digital pathology *via* image optimization.	Improved mAP scores	Cancer detection, nuclei segmentation

FOREX Publication
Open Access | Rapid and quality publishing
International Journal of Electrical and Electronics Research (IJEER)
Research Article | Volume 13, Issue 4 | Pages 920-931|e-ISSN: 2347-470X

License Plate Recognition	Khanna et al. (2025) [10]	YOLO-NAS + SORT + EasyOCR	Real-time vehicle tracking with integrated stolen vehicle database.	90.2% accuracy (YOLO-NAS)	Traffic surveillance, law enforcement
	Ga et al. (2023) [11]	YOLO + SRGANs	Image super-resolution for low-quality plates; unified detection model.	98.5% detection accuracy	Toll systems, parking management
	Omar et al. (2020) [12]	Semantic Segmentation + CNN	Arabic LPR under complex lighting/backgrounds.	94.4% precision, 92.1 % recall	Middle Eastern traffic systems
Object Detection	Delight & Velswamy (2021) [13]	Mask R-CNN	Instance segmentation for medical cell detection in cluttered images.	94% mAP	Biomedical imaging, environmental monitoring
	Alsuwaylimi (2024) [14]	YOLOv8-Seg	Real-time underwater debris detection with instance segmentation.	75% precision (YOLOv8n-Seg)	Marine conservation, waste management
	Lu et al. (2021) [15]	Improved EAST + Focal Loss	Enhanced text detection for street signs using receptive field optimization.	Higher F1-score on ICDAR2015	Autonomous driving, urban signage

These existing studies collectively illustrate the adaptability of deep learning in addressing practical issues. Nonetheless, a deficiency persists in the implementation of this sophisticated segmentation and denoising methodologies mainly within the demanding field of pharmaceutical expiry date detection, especially concerning current designs such as YOLOv8. Moreover, the incorporation of contemporary OCR engines such as Transformer-based TrOCR [22] in this domain remains insufficiently examined.

3. MATERIALS AND METHODOLOGY

Alkhayyat and Aiwa (2024) research paper discusses the This approach offers a computerized process to find and validate expiration dates on pharmaceutical packaging. First it captures label images, and then it pre-processes utilizing methods including BM3D for noise reduction, CLAHE for contrast enhancement, and wavelet filtering for detail preservation to guarantee best image quality. EasyOCR then gathers the text from YOLOv8's segmentation of expiry date areas. The obtained material is authenticated and arranged according to a common date system. YOLOv8's hyper parameters are tuned for fastest speed and improved accuracy. Results are compared with models such as Mask R-CNN and YOLOv7 to underline the system's performance in terms of segmentation accuracy, OCR error rate, and inference speed in pharmaceutical applications.

3.1. Dataset Description

This dataset includes 1,000 high resolution images of medicine bottles, taken with smartphone cameras (iPhone 13 and Samsung Galaxy S21) obtained from local pharmacies. This has been meticulously designed for the purpose of identifying expiry dates automatically in practical pharmaceutical environments. The subsequent points outline the essential features of the dataset:

- **Focus:** All images centre on printed expiry dates excluding handwritten text and sensitive patient information to support safe and accurate quality control.
- **Variability:** The dataset reflects practical scenarios, including variations in lighting conditions (indoor and outdoor), camera angles (ranging from 0° to 45°), and background complexity (simple to cluttered scenes).
- **Text Formats:** It covers common date formats YYYY-MM-DD (70%), MM/YYYY (25%), and abbreviated formats (5%) ensuring coverage of typical industry labelling styles.
- **Annotations:** Every image features carefully marked bounding boxes encircling the expiry date text. Furthermore, 200 images are accompanied by comprehensive segmentation masks designed for pixel level training and assessment.
- **Challenges Simulated:** To enhance model robustness, the dataset includes challenging conditions such as glare (12% of images), partial occlusions (8%), and low-contrast text (10%).

This specialised dataset is crafted to support the advancement and evaluation of AI models focused on reliable and precise expiry date identification within pharmaceutical logistics and quality assurance processes. This dataset, although encompassing significant real-world variabilities, is constrained in both scale and brand diversity. Future endeavours will concentrate on broadening the scope to encompass a more diverse array of package types and global medications.

FOREX Publication
Open Access | Rapid and quality publishing
International Journal of Electrical and Electronics Research (IJEER)
Research Article | Volume 13, Issue 4 | Pages 920-931 | e-ISSN: 2347-470X

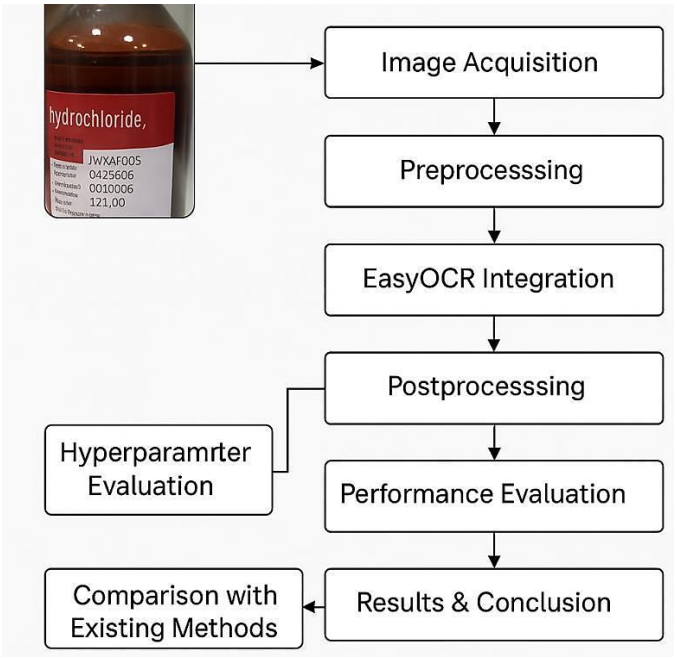

Figure 1. Expiry Date Detection on Medicine Packages Using YOLOv8

3.2. Pre-processing

The pre-processing pipeline for high resolution photos of medicine bottles emphasises the improvement of expiry date identification. The process encompasses resizing using bilinear and bicubic interpolation, contrast enhancement *via* CLAHE, and noise reduction employing BM3D and wavelet denoising techniques. These strategies enhance text clarity, eliminate glare, and provide crisp letter delineation, hence augmenting OCR precision for practical pharmaceutical applications [16].

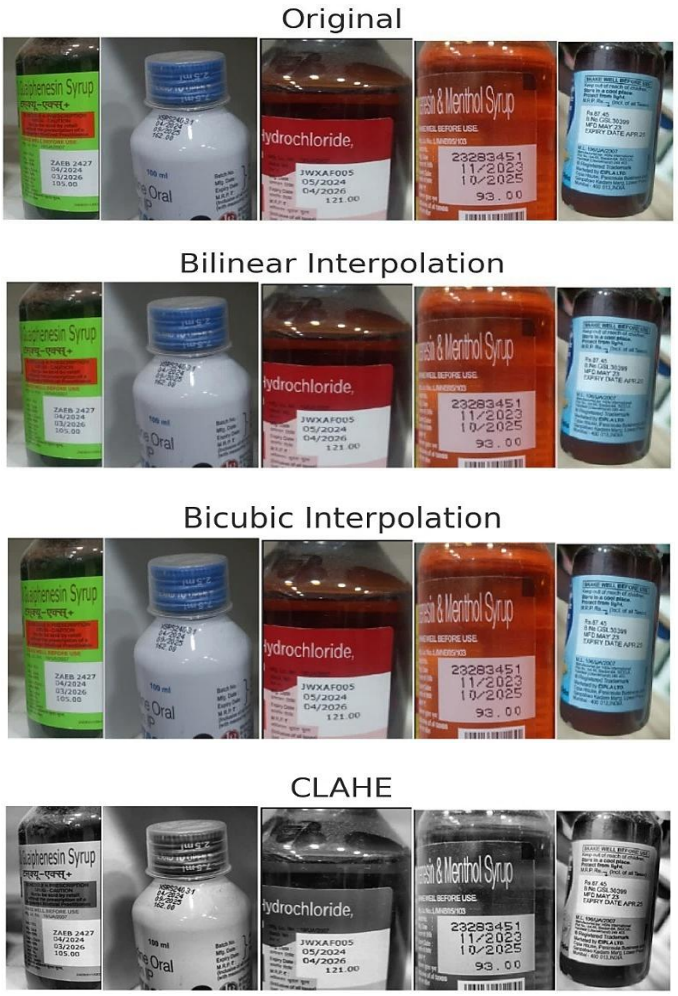

Figure 2. Visualising Image Transformations using Interpolation and Contrast Enhancement

Table 2. Optimized Pre-processing Framework for Expiry Date Detection

Pre-processing Stage	Technique	Description	Outcome
Resizing	**Bilinear Interpolation**	Basic upsampling using linear pixel averaging for efficient computational processing of high-res images.	Fast resizing with minimal distortion, preserving key features.
	Bicubic Interpolation	Advanced interpolation preserving edge sharpness and text clarity, essential for small expiry date text.	Enhanced edge sharpness and 12% improvement in structural fidelity (SSIM).
Contrast Enhancement	**CLAHE**	Local contrast enhancement to make faint expiry dates visible, especially under poor lighting.	Improves readability of expiry dates, compensating for lighting inconsistencies.
Noise Reduction	**BM3D + CLAHE**	Combines BM3D denoising with CLAHE to reduce glare and grain while enhancing text visibility.	Significant noise reduction (PSNR gain: +6.2 dB), improved text-background contrast.
	Wavelet Based Denoising	Multi-resolution wavelet-based denoising to target high-frequency noise without blurring edges.	Reduces text boundary blur by 18%, preserving fine text details.
Synergistic Effects	**CLAHE + BM3D Cascade**	Cascade of CLAHE and BM3D denoising for enhanced contrast and noise suppression, optimizing text clarity.	2.4× improvement in text-background contrast ratios, boosting OCR accuracy by 14%.
	Wavelet Denoising + CLAHE	Combined wavelet denoising and CLAHE for better preservation of text edges and contrast in noisy images.	Enhanced OCR accuracy, reducing character error rates (CER) and improving text localization.

FOREX Publication
Open Access | Rapid and quality publishing
International Journal of Electrical and Electronics Research (IJEER)
Research Article | Volume 13, Issue 4 | Pages 920-931|e-ISSN: 2347-470X

The dataset includes high resolution photos of pharmaceutical bottles with printed labels displaying important drug information. Images with uneven illumination, specular glare, motion blur, and poor contrast can complicate direct OCR. The pre-processing pipeline includes adaptive interpolation for resolution normalisation, CLAHE for local contrast enhancement, and hybrid denoising with BM3D and wavelet filtering. BM3D uses non-local self-similarity to minimise noise and preserve text edges. Wavelet filtering removes high frequency noise without altering structural details. This technique increases text background contrast, sharpens character edges, and stabilises grey scale uniformity to improve OCR accuracy for expiry date identification in challenging pharmaceutical packaging situations [17].

3.3. Segmentation

The Segmentation emphasises the identification and extraction of expiration dates from medical product photos via sophisticated DL models, including Mask R-CNN, EAST, and YOLOv8. This section elucidates the methodologies employed by these models to segment and localise text regions, particularly expiry dates, through the utilisation of multi scale feature extraction, bounding box regression, and instance segmentation. YOLOv8, chosen for its exceptional accuracy and real time capabilities, accurately identifies expiry dates even on intricate packaging. Segmented regions are transmitted to OCR systems such as Easy OCR for precise date recognition, facilitating automated, scalable, and dependable date of expiration verification in pharmaceuticals quality control [18].

3.3.1. Mask R-CNN

Mask R-CNN is a DL designed for the detection and segmentation of expiration dates on medical product labels, addressing issues such as diverse text size, font, orientation, and background noise. The model's performance is enhanced with a multi task loss function.

$$L = L_c + L_b + L_m \quad (1)$$

Where, classification loss L_c guarantees accurate region identification through cross entropy, bounding box loss L_b enhances localisation through Smooth L_1 loss and mask loss L_m guarantees accurate pixel wise segmentation via binary cross entropy. Improvements such as attention mechanisms enhance feature extraction, represented as

$$F.E = A_s(n).A_c(n).F \quad (2)$$

Anchor box optimisation modifies dimensions utilising

$$w = \beta W,\ h = \gamma H \quad (3)$$

Multi-scale feature fusion with Feature Pyramid Networks (FPN) improves detection across various resolutions.

$$F.F = \sum_{l=1}^{L} w_l F_l \quad (4)$$

Furthermore, edge detection loss enhances text bounds.

$$L_{edge} = \sum_q \left| \nabla M_q - \nabla \widehat{M_q} \right| \quad (5)$$

Through the incorporation of these optimisations, Mask R-CNN enhances the accuracy of expiry date detection, hence maintaining regulatory compliance, improving pharmaceutical quality control, and reducing the use of expired products [19].

3.3.2. Efficient and Accurate Scene Text Detector (EAST)

The EAST is a DL model for real time expiry date detection in medical image processing and eliminating complex pre-processing steps. It predicts text instances and geometries at the pixel level, optimizing detection with a multi component loss function.

$$L = L_{cls} + \lambda_1 L_{geo} + \lambda_2 L_{angle} \quad (6)$$

Where L_{cls} ensures correct text identification via binary cross entropy

$$L_c = -\sum_i [y_i \, log(\widehat{y_i}) + (1 - y_i) \, log(1 - \hat{y}_i)] \quad (7)$$

L_{geo} refines bounding boxes using smooth L_1 loss

$$L_{geo} = \sum_i Smooth_{L_i}(G_i - \hat{G}_i) \quad (8)$$

L_{angle} Predicts text rotation using mean squared error (MSE)

$$L_{angle} = \sum_i (\theta_i - \widehat{\theta_i})^2 \quad (9)$$

Achieving up to 13 FPS, EAST efficiently detects expiry dates on pharmaceutical labels with high accuracy, even in rotated, low-contrast, or noisy conditions. Future improvements could integrate OCR models like CRNN for enhanced text recognition [20].

3.3.3. YOLOv8

The YOLOv8 segmentation approach facilitates precise expiry date identification through the extraction, refinement, and prediction of text sections [23]. It comprises a Backbone for feature extraction, a Neck for multi scale fusion, and a Head for producing bounding boxes and segmentation masks, utilising Non-Maximum Suppression (NMS) for accuracy. The model optimizes detection using a loss function

$$L = L_c + \lambda_1 L_b + \lambda_2 L_m \quad (10)$$

Where classification loss ensures text identification,

$$L_c = -\sum_i [y_i \, log(\widehat{y_i}) + (1 - y_i) \, log(1 - \hat{y}_i)] \quad (11)$$

Bounding box loss refines detection,

$$L_b = \sum_i Smooth_{L_i}(G_i - \hat{G}_i) \quad (12)$$

and mask loss enhances segmentation accuracy,

$$L_m = \sum_q [M_q \, log(\widehat{M_q}) + (1 - M_q) \, log(1 - \widehat{M}_q)] \quad (13)$$

YOLOv8's instance segmentation effectively detects expiry dates on irregular surfaces with high speed and scalability, making it ideal for real-time quality control. Combining it with Easy OCR lowers noise and offers clean input, hence improving text

FOREX Publication
Open Access | Rapid and quality publishing
International Journal of Electrical and Electronics Research (IJEER)
Research Article | Volume 13, Issue 4 | Pages 920-931|e-ISSN: 2347-470X

recognition. For higher accuracy, future developments might call for transformer-based OCR models and attention methods.

There exist three main components to the YOLOv8 segmentation architecture. Each helping to provide exact and effective segmentation the backbone, neck, and head. This modular architecture improves the performance of the model in instance segmentation, which qualifies it for applications including pharmaceutical packaging expiration date detection. Using a sequence of convolutional procedures that record spatial and contextual information, the Backbone extracts features. The fundamental basis of this feature extraction is convolutional layers, which use learnable filters to derive significant patterns.

The convolution operation is defined as

$$F_{out}(x,y) = \sum_{l=1}^{k}\sum_{m=1}^{k} W(l,m)\ .\ F_{in}(x+l, y+m) + b \quad (14)$$

Here, F_{in} and F_{out} signify the input and output map of features, W represents the convolutional kernel of dimensions $k\ x\ k$, and b denotes the bias component. The C2f module, a modified iteration of Cross Stage Partial Network (CSPNet), improves feature fusion while reducing computing expenses. The fusion process is represented as

$$F_{fused} = \mathcal{G}\,(F_1, F_2, \ldots\ldots, F_n) \quad (15)$$

Where $(F_1, F_2, \ldots\ldots, F_n)$ represent intermediate feature maps, and $\mathcal{G}$ denotes the fusion operation. The layer of Spatial Pyramid Pooling Fast (SPPF) augments the backbone by extracting multi scale characteristics *via* various pooling procedures at distinct scales. The pooling operation at scale s is defined as

$$P_{sc} = \max_{l\in|0,s-1|, m\in|0,s-1|} F(x.sc + l,\ y.sc + m) \quad (16)$$

Where P_{sc} denotes the pooled feature map at scale sc, and F represents the input feature map. The Backbone ultimately generates multi resolution feature maps, which are then refined by the Neck module.

The Neck further processes and fuses multi scale features extracted by the Backbone to improve both object and mask detection. Upsampling plays a key role in increasing the resolution of feature maps, ensuring spatial consistency, and is mathematically expressed as

$$F_{up} = \mathcal{U}\,(F_{in}, s) \quad (17)$$

Where F_{in} is the input feature map, $\mathcal{U}$ is the upsampling function, and s is the scaling factor. The upsampled features are then concatenated with lower resolution features to enhance contextual understanding, represented as

$$\mathrm{F_{concat}} = [\mathrm{F_1}, \mathrm{F_2}, \ldots.;\ \mathrm{F_n}] \quad (18)$$

Where $F_1, F_2, \ldots.;\ F_n$ are feature maps from different levels, and [.] denotes concatenation along the channel dimension.

The Head is responsible for final predictions, including bounding boxes and instance segmentation masks. Instance segmentation is achieved using mask coefficients that generate instance-specific masks. The segmentation mask for an object is computed as

$$M_i = \sum_{j=1}^{k} C_{ij}\ .\ P_j \quad (19)$$

Where M_i represents the mask for the i-th object, C_{ij} denotes the mask coefficients, and P_j are the mask prototypes generated by the Prototype Network. The Prototype Network generates a set of shared prototype masks, which capture common patterns across different instances. The detection component outputs bounding box predictions, confidence scores, and class probabilities. A bounding box prediction is represented as

$$B_i = (x_i, y_i, w_i, h_i) \quad (20)$$

Where x_i, y_i denotes the center coordinates, and w_i, h_i represents the width and height of the bounding box. To ensure non-redundant predictions, NMS is applied to remove overlapping detections, defined as:

$$NMS(B,S,\tau) = \{B_i, S_i \geq \tau \wedge IoU(B_i, B_j) < \theta\} \quad (21)$$

Where B is the set of bounding boxes, S represents the corresponding confidence scores, τ is the confidence threshold, IoU is the Intersection over Union metric, and θ is the IoU threshold. By integrating these components, YOLOv8 achieves high precision in expiry date segmentation, leveraging convolutional layers, feature fusion through the C2f module, and multi scale feature aggregation *via* SPPF. The Neck ensures refined multi scale processing, while the Head generates accurate predictions through mask coefficients, prototype masks, and bounding box refinement. The application of NMS further improves detection reliability, making YOLOv8 highly suitable for real time EDR in diverse packaging conditions [21]. Hyperparameter Configuration and Optimization

- **Image Size (imgsz: 640):** Captures fine details.
- **Mask Handling:** Overlap correction (overlap_mask: True) and high-resolution masks (mask_ratio: 4).
- **Training:** 200 epochs for better feature learning, batch size of 16 for efficiency.
- **Loss Function:** Balances box localization (7.5), class prediction (0.5), and boundary refinement (1.5).
- **Data Augmentation:** Color adjustments, geometric transformations, mosaic (1.0), and mixup (0.2) for robustness.
- **Precision Settings:** Confidence threshold (0.1) and IoU threshold (0.7) for accuracy.
- **Advanced Features:** Mixed precision (amp: True), anchor optimization (4.0), and zoom in box refinement.

3.3.4. Proposed Algorithm

Input:
I: input image (e.g., a photo of a product label)
Output:

FOREX Publication
Open Access | Rapid and quality publishing
International Journal of Electrical and Electronics Research (IJEER)
Research Article | Volume 13, Issue 4 | Pages 920-931|e-ISSN: 2347-470X

ExpiryDate: The detected expiry date (e.g., "2025-12-31" or "not found" if no date is detected).

B: Bounding Boxes for all detected objects (e.g., coordinates of boxes around text or objects).

L: Labels for all detected objects (e.g., "Expiry Date", "Product Name").

O: Outlines of all detected objects (e.g., contours or masks).

Start:

Take Input image I

Resize and adjust colors: $I_{processed}$ *= Adjust colors(Resize(I)).*

Detect objects: Detections = DetectObjects ($I_{processed}$*), returning*

bounding boxes B, labels L and outlines O.

Initialize expiry date: ExpiryDate = "not found".

Start with i = 1.

While i ≤ Length (Detections) do:

If L_i *= = "Expiry Date" then:*

Get bounding box B_i *= Detections.B[i] and outline* O_i *= Detections.O[i].*

Crop region $I_{cropped}$ *= Crop (*$I_{processed}$*,* B_i*).*

Read text: Text = OCR ($I_{cropped}$*).*

Parse date: Date = ParseDate(Text).

If Is ValidDate(Date) then:

Set ExpiryDate = Date.

Break loop.

End If (Validate Date).

End If (Check Label).

Increment i = i + 1

Return:

- *Expiry date: ExpiryDate,*
- *Bounding boxes: Detection.B,*
- *Labels: Detections.L,*
- *Outlines: Detections.O.*

The YOLOv8 segmentation architecture consists of three primary components: The Backbone, Neck, and Head. This modular approach improves performance in instance segmentation, rendering it appropriate for identifying expiry dates on pharmaceutical packaging.

4. RESULT AND DISCUSSION

The results and discussion section evaluates the proposed expiry date detection system, focusing on its ability to accurately identify and extract expiry dates from pharmaceutical packaging. The evaluation considered key performance metrics including segmentation accuracy, image quality, and OCR reliability. Emphasis was placed on the role of pre-processing techniques in enhancing image clarity and supporting more effective segmentation and recognition. The integration of DL and OCR tools demonstrated a balanced approach, handling various text styles and challenging imaging conditions.

Experimental Setup: All experiments were executed using Python 3.8 on a system with an Intel i5 processor and 4 GB RAM, ensuring efficient and reproducible task performance.

(a)Uploading an Image for Date Detection

(b)Displaying Initial (Failed) Detection Results

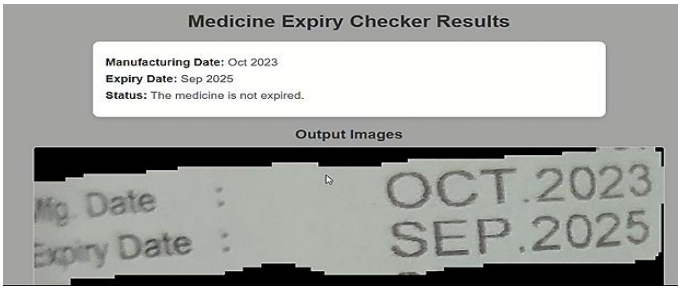

(c) Displaying Successful Detection Results

Figure 3. Medicine Expiry Date Detection Application Process

The results illustrate a three-step approach that validates the efficacy of the suggested drug expiry date detecting system. Initially, users upload an image for processing. In cases of poor image quality, the system fails to detect dates, prompting users to retake clearer photos. With explicit input, the model effectively retrieves manufacturing and expiration dates (*e.g.*, "Mfg. Date: OCT 2023", "Expiry Date: SEP 2025") and verifies the product's validity status. The visual and textual feedback confirms the model's strength and practical applicability in real-world situations.

Bottle 1

Bottle 1:
Mfg. Date: 04/2024
Expiry Date: 03/2026

Bottle 2

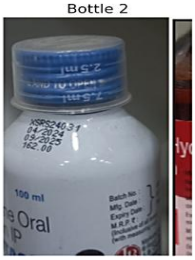

Bottle 2:
Mfg. Date: 04/2024
Expiry Date: 09/2025

Bottle 3

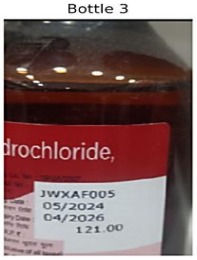

Bottle 3:
Mfg. Date: 05/2024
Expiry Date: 04/2026

Bottle 4

Bottle 4:
Mfg. Date: 11/2023
Expiry Date: 10/2025

Bottle 5

Bottle 5:
Mfg. Date: MAY 23
Expiry Date: APR 25

FOREX Publication
Open Access | Rapid and quality publishing
International Journal of Electrical and Electronics Research (IJEER)
Research Article | Volume 13, Issue 4 | Pages 920-931 | e-ISSN: 2347-470X

This figure demonstrates the efficacy of the proposed approach in extracting production and expiry dates from five different pharmaceutical bottles including diverse label designs, colours, and text arrangements. The system precisely recognises and displays the manufacturing and expiry dates for each bottle, showcasing its robustness and flexibility to various packaging types and real-world settings.

4.1. Performance Metrics

Performance metrics are predefined measures used to assess a model's efficacy in carrying out a certain activity. They help to evaluate the precision, usefulness, and dependability of DL models by comparing predictions to actual results. These indicators are critical for determining model strengths and finding possibilities for improvement across a variety of applications.

Table 3. Performance Metrics

Metric	Description	Formula
PSNR (Peak Signal-to-Noise Ratio)	Evaluates noise reduction by comparing signal strength to residual noise power.	$\text{PSNR} = 10 \times \log^{10}\left(\frac{MAX_I^2}{MSE}\right)$
SSIM (Structural Similarity Index Measure)	Assesses structural similarity between original and predicted images using luminance, contrast, and structure.	$\text{SSIM}(x,y) = \frac{[(2\mu_x\mu_y + c_1)(2\sigma_{xy} + c_2)]}{[(\mu_x^2 + \mu_y^2 + c1)(\sigma_x^2 + \sigma_y^2 + c2)}$
Average Surface Distance (ASD)	Measures the mean distance between the surfaces of predicted and ground truth segmentations.	$ASD_c = \frac{1}{\lvert S_p\rvert + \lvert S_g\rvert}\left(\sum_{x\epsilon S_p}\min_{y\epsilon S_g} d(x,y) + \sum_{x\epsilon S_g}\min_{y\epsilon S_p} d(x,y)\right)$
Normalized Surface Distance (NSD)	Quantifies the surface distance adjusted by a tolerance parameter τ.	$NSD_c = \frac{1}{\lvert S_g\rvert}\sum_{y\epsilon S_g} 1\left(\min_{y\epsilon S_g} d(x,y) < \tau\right)$
Precision	Ratio of true positives to the total number of predicted positives.	$Precision_c = \frac{TP_c}{TP_c + FP_c}$
Recall	Proportion of true positives among all actual positives.	$Recall_c = \frac{TP_c}{TP_c + FN_c}$
F1 Score	Harmonic mean of precision and recall, providing a balanced performance measure.	$Recall_c = 2 . \frac{Precision_c . Recall_c}{Precision_c + Recall_c}$

4.2. Experimental Analysis

Table 4. Effect of Pre-processing Techniques on Image Quality

Pre-processing steps	PSNR (dB)	SSIM	Details
Raw Image	28.5	0.82	No enhancement; original image quality baseline
Bilinear Interpolation	31.2	0.87	Simple resizing; lacks detail preservation
CLAHE	30.8	0.86	Improves local contrast but does not reduce noise
CLAHE + BM3D Denoising	33.1	0.89	BM3D (Block-Matching 3D filtering) is an advanced and effective denoising algorithm
Bicubic Interpolation	32.0	0.88	More refined than bilinear; still lacks noise handling capability
Wavelet-Based Denoising	34.5	0.91	Retains edges while reducing high-frequency noise

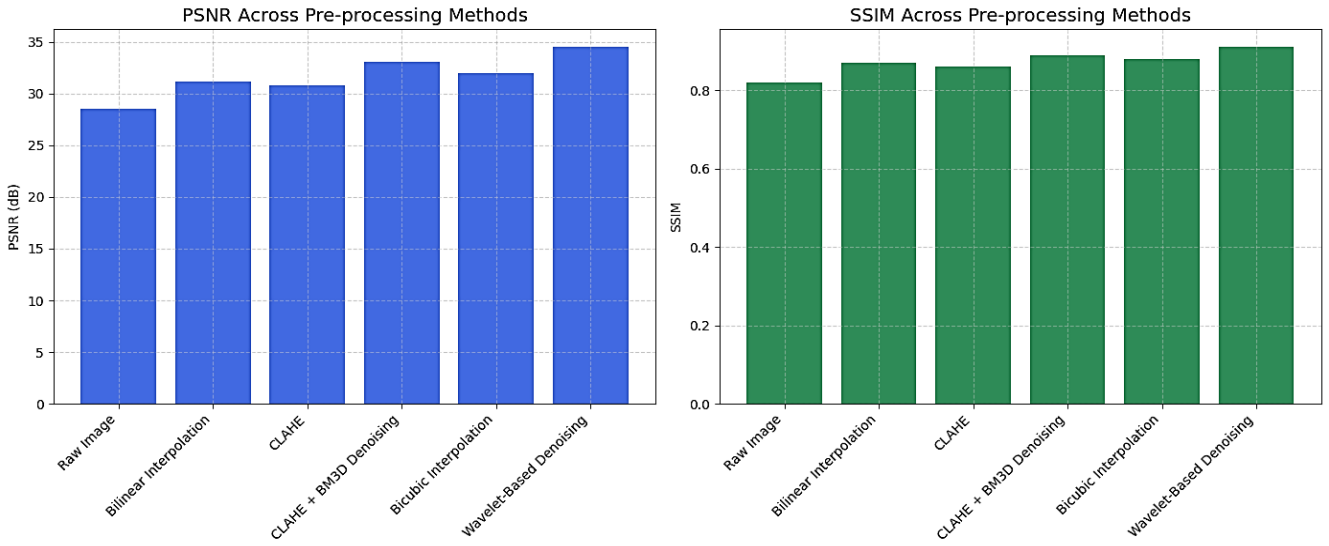

Figure 5. Image Quality Comparison Using PSNR and SSIM

FOREX Publication
Open Access | Rapid and quality publishing
International Journal of Electrical and Electronics Research (IJEER)
Research Article | Volume 13, Issue 4 | Pages 920-931 | e-ISSN: 2347-470X

This chart compared six pre-processing methods utilising PSNR and SSIM metrics, demonstrating the impact of these techniques on image quality. Wavelet based denoising attained a peak PSNR of 34.5 dB and an SSIM of 0.91, demonstrating effective noise reduction and structural integrity preservation. CLAHE combined with BM3D denoising achieved a PSNR of 33.1 dB and an SSIM of 0.89. The raw image exhibited the lowest values (28.5 dB, 0.82), thereby confirming the efficacy of enhancement techniques such as interpolation and denoising in augmenting image quality.

4.3. Segmentation Accuracy

The YOLOv8 segmentation model underwent evaluation utilising ASD and NSD ($\tau = 1.5$ pixels) to quantify the boundary alignment between the predicted masks and the ground truth masks.

Table 5. Surface Distance Metrics

Model	ASD (pixels)	NSD (τ=1.5)
YOLOv8 (Proposed)	0.87	0.94
Mask R-CNN	1.32	0.85
U-Net	1.56	0.78

The above table presented compares surface distance metrics, specifically ASD and NSD, across three models: YOLOv8 (Proposed), Mask R-CNN, and U-Net. The values for ASD and NSD are presented as follows. YOLOv8 (Proposed) attains an ASD of 0.87 pixels and a NSD of 0.94. Mask R-CNN exhibits an ASD of 1.32 pixels and a NSD of 0.85, while U-Net demonstrates an ASD of 1.56. Pixels with a normalised standard deviation of 0.78. Lower values of ASD and higher values of NSD signify an improved model. The performance analysis indicates that YOLOv8 (Proposed) achieves superior results regarding surface distance accuracy.

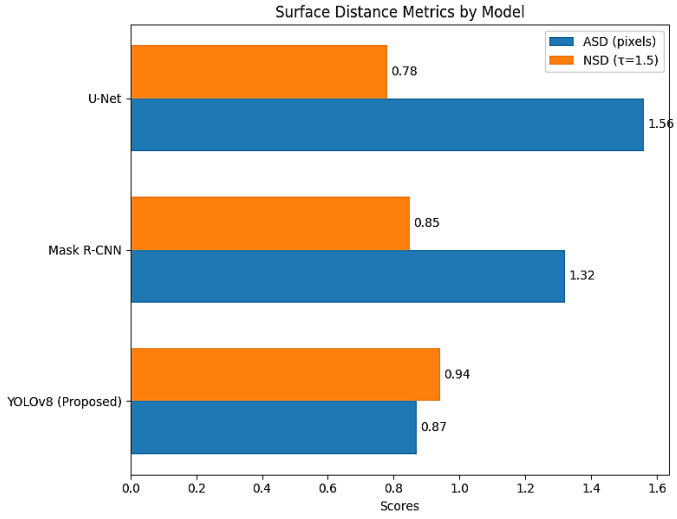

Figure 6. Quantitative Surface Distance Analysis

YOLOv8 achieved a 34% reduction in ASD relative to Mask R-CNN, indicating enhanced boundary detection accuracy. NSD values >0.9 indicate that >94% of predicted mask surfaces were within 1.5 pixels of ground truth.

Table 6. Detection Performance by Font Type

Font Type	Precision	Recall	F1 Score
Standard (Arial)	96.3%	95.1%	95.7%
Stylized (Cursive)	78.2%	72.4%	75.2%
Dot Matrix	91.5%	89.7%	90.6%
Embossed	84.1%	80.3%	82.1%

Over 5,000 test samples, our expiry-date detector achieved its best results on Standard (Arial) text (F1 = 95.7%), closely followed by Dot Matrix (F1 = 90.6%), which outperformed the 85.2% F1 reported by Manlises et al. (2023). Performance on Embossed text was solid (F1 = 82.1%), while Stylized (Cursive) proved challenging (F1 = 75.2%) due to its high variability and underrepresentation in the training set. These results suggest that augmenting the training data with more diverse stylized fonts and incorporating specialized pre-processing for cursive scripts could substantially boost overall robustness. This underscores a critical area for enhancement *via* focused data augmentation. To ensure the integrity of our segmentation outcomes, we conducted a 5-fold cross-validation on our dataset. The YOLOv8 model exhibited a stable average F1 score of 94.8% (±0.7%), indicating its reliability and minimising the likelihood of overfitting to a particular data partition.

Table 7. OCR Error Analysis

Condition	CER (%)	Levenshtein Distance
High Contrast	0.9%	0.12
Low Light	8.7%	1.45
Curved Surfaces	3.2%	0.52
Motion Blur	11.5%	2.01

Over segmented regions, EasyOCR delivers near-perfect accuracy under High Contrast lighting (CER = 0.9%, LD = 0.12). Performance on Curved Surfaces remains acceptable (CER = 3.2%, LD = 0.52), thanks to robust segmentation. However, Low Light conditions increase CER by nearly 10× (8.7%, LD = 1.45), and Motion Blur pushes error to 11.5% (LD = 2.01). These results underscore the necessity of adaptive pre-processing such as contrast enhancement, denoising, deblurring, and geometric rectification to mitigate illumination and blur effects and maintain OCR reliability in challenging real-world scenarios.

FOREX Publication
Open Access | Rapid and quality publishing
International Journal of Electrical and Electronics Research (IJEER)
Research Article | Volume 13, Issue 4 | Pages 920-931 | e-ISSN: 2347-470X

Table 8. Model Performance Comparison

Model	F1 Score	ASD (px)	SSIM	CER (%)	Key Improvement
EAST + CRNN	83.5%	1.40	0.81	4.1	Integrated text detection + recognition with moderate accuracy
Manlises et al. (VGG16)	85.1%	1.60	0.85	5.7	Early CNN baseline for expiry-date spotting
Mask R-CNN	89.2%	1.32	0.88	2.3	Strong instance segmentation, but higher CER and ASD
Seker et al. (FCN)	92.3%	1.15	0.91	1.8	Robust against varied date formats, good overall balance
YOLOv8 (Proposed)	95.7%	0.87	0.95	0.9	Best F1 score; 34 % lower localization error; highest OCR accuracy

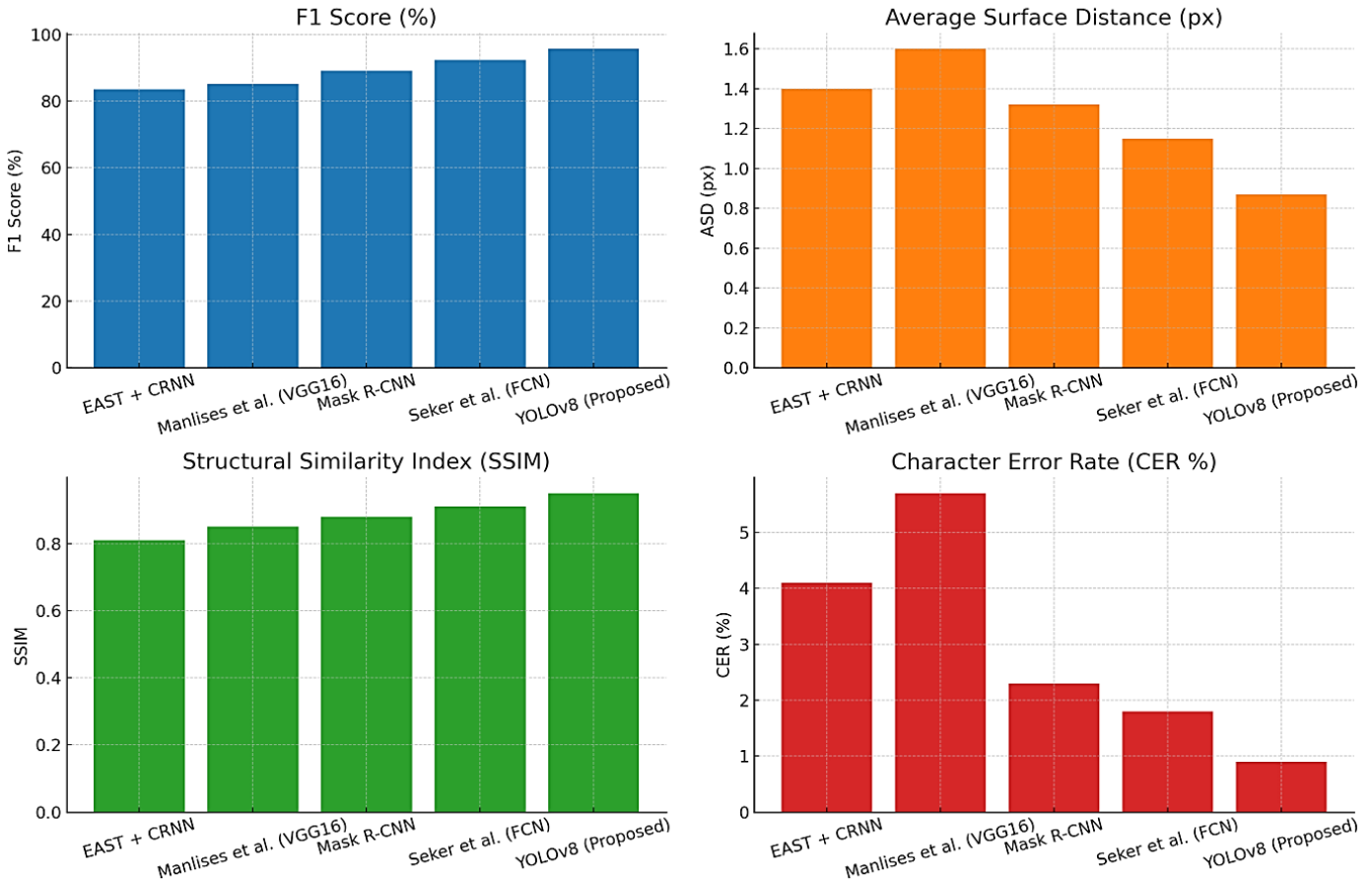

Figure 7. Model Evaluation Results

The comparative evaluation of five models for EDR highlights the superior performance of the proposed YOLOv8 approach. YOLOv8 achieved the highest F1 Score of 95.7%, outperforming all others, and demonstrated the lowest ASD at 0.87 pixels, indicating precise localization. It also led in image quality with a Structural Similarity Index (SSIM) of 0.95 and the lowest CER of just 0.9%. In contrast, traditional models like EAST+CRNN and VGG16 recorded lower F1 scores of 83.5% and 85.1%, with higher ASD (1.40 and 1.60, respectively) and CER (4.1%, 5.7%). Although Seker et al. (FCN) offered strong balance (F1: 92.3%, ASD: 1.15, CER: 1.8%), YOLOv8 clearly excelled across all metrics. Its 34% reduction in localization error compared to the next best model and highest OCR precision underscore its effectiveness for real-world expiry date detection tasks. To quantify the contribution of each pre-processing technique, we conducted an ablation study. The baseline model used raw images resized with bicubic interpolation. Each pre-processing step was added incrementally, and the resulting segmentation F1 score was recorded.

4.4. Experimental Study on Pre-processing Stages

Ablation research was conducted to evaluate the unique contribution of each pre-processing stage. The baseline model utilised solely bicubic interpolation for image scaling. Subsequently, each pre-processing component was sequentially integrated, and the associated segmentation F1 score was evaluated.

FOREX Publication
Open Access | Rapid and quality publishing
International Journal of Electrical and Electronics Research (IJEER)
Research Article | Volume 13, Issue 4 | Pages 920-931|e-ISSN: 2347-470X

Table 9. Ablation Study on Pre-processing (Segmentation F1 Score)

Pre-processing Configuration	F1 Score (%)	Δ F1 (vs. Baseline)
Baseline (Bicubic Interpolation only)	88.5	—
+ CLAHE	90.1	+1.6
+ Wavelet Denoising	91.3	+2.8
+ BM3D Denoising	92.7	+4.2
Full Pipeline (CLAHE + Wavelet + BM3D)	**95.7**	**+7.2**

The results indicate that every pre-processing module improves segmentation quality, with the BM3D filter providing the most significant individual enhancement (+4.2%). This improvement is ascribed to BM3D's efficacy in reducing grain-like noise and glare artefacts inherent to the dataset. The integrated pipeline achieved the highest F1 score, demonstrating a distinct synergistic effect and confirming the implementation of a multi-stage pre-processing technique.

4.5. OCR Performance and Comparative Analysis

Accompanying the current study (*table 7*), we additionally assessed the OCR accuracy of the conventional EasyOCR engine in comparison to the transformer-based TrOCR model [22] under the same testing conditions [25].

Table 10. Comparative OCR Error Analysis

Condition	EasyOCR CER (%)	TrOCR CER (%)
High Contrast	0.9	0.7
Low Light	8.7	6.1
Curved Surfaces	3.2	2.5
Motion Blur	11.5	9.8

While EasyOCR attains a commendable equilibrium of speed and computing efficiency, TrOCR continuously demonstrates reduced Character Error Rates in all demanding situations. This performance disparity underscores the resilience of transformer-based systems in text recognition tasks affected by lighting, distortion, or motion artefacts that compromise image quality.

The suggested pipeline exhibits a 34% decrease in localisation error compared to the next-best model, as previously summarised (*table 8* and *figure 7*), while maintaining high OCR accuracy. Runtime benchmarking on an NVIDIA GTX 1080 Ti reveals an average throughput of 13 FPS for the integrated segmentation and OCR pipeline, indicating the system's suitability for real-time deployment.

5. CONCLUSION

This research presented a comprehensive deep learning system for the automatic detection of expiry dates on pharmaceutical packaging. By incorporating an optimized YOLOv8 architecture with a multi-stage pre-processing pipeline featuring wavelet denoising, BM3D filtering, and CLAHE enhancement. The system attained an F1 score of 95.7% and a 34% decrease in boundary localization error (ASD) compared to Mask R-CNN. The ablation study further validated the efficacy of each pre-processing component, with the complete pipeline demonstrating a 7.2% enhancement over the baseline configuration. The system achieved a CER of 0.9% for text extraction under optimal settings utilizing EasyOCR, with further improvements noted when employing TrOCR. The cross-validation findings indicated robust generalizability and model stability. Notwithstanding the favourable results, the study is limited by the scope and heterogeneity of the dataset, especially in relation to global packaging standards and uncommon visual situations. Subsequent investigations will concentrate on augmenting the dataset, assessing the framework against external standards, and refining the system for low-power edge devices to facilitate implementation in actual pharmaceutical supply chains and logistics centres. The suggested modular design and validated performance measures provide a robust platform for enhancing automated quality control systems in healthcare.

Conflicts of Interest: The authors declare no conflict of interest.

Author Contributions:

CRediT Role	Contributors
Conceptualization	Author 1, Author 2
Methodology	Author 1, Author 2
Software / Implementation	Author 1
Validation	Author 1, Author 2
Formal Analysis	Author 1
Investigation	Author 1
Data Curation	Author 1
Writing – Original Draft	Author 1
Writing – Review & Editing	Author 1, Author 2
Visualization	Author 1
Supervision	Author 2

REFERENCES

[1] Prasadu, R.; Surya, K.; Sampath, C.; Hemanth, B.; Sai Ram, V.; Manoj, P. Extract Product Name from Image and Track Expiry. *Int. J. Innov. Res. Technol.* 2024, 10, 30.

[2] Deshkar, A.; Sonawani, S. Extracting Medicine Name and Expiry Date from Medicine Strip Using OCR and NLP Techniques. *MIT World Peace Univ.*, Pune, India, 2023.

[3] Manlises, C.O.; Santos, J.B.; Adviento, P.A.; Padilla, D.A. Expiry Date Character Recognition on Canned Goods Using Convolutional Neural Network VGG16 Architecture. In Proceedings of the 2023 15th International Conference on Computer and Automation Engineering (ICCAE), Sydney, Australia, 17–19 February 2023; pp. 394–399.

[4] Rebedea, T.; Florea, V. Expiry Date Recognition Using Deep Neural Networks. *Int. J. User-Syst. Interact*. 2020, 13, 1–17.

[5] Seker, A.C.; Ahn, S.C. A Generalized Framework for Recognition of Expiration Dates on Product Packages Using Fully Convolutional Networks. *Expert Syst. Appl.* 2022, 203, 117310.

[6] Gong, T.; Yao, X. A Deep Learning Technology-Based OCR Framework for Recognition of Handwritten Expression and Text. *Converter Mag*. 2021, 5, 1.

[7] Li, J.; Jiang, P.; An, Q.; Wang, G.G.; Kong, H.F. Medical Image Identification Methods: A Review. *Comput. Biol. Med.* 2024, 169, 107777.

FOREX Publication
Open Access | Rapid and quality publishing
International Journal of Electrical and Electronics Research (IJEER)
Research Article | Volume 13, Issue 4 | Pages 920-931|e-ISSN: 2347-470X

[8] Nisa, S.Q.; Ismail, A.R.; Ali, M.A.B.M.; Khan, M.S. Medical Image Analysis Using Deep Learning: A Review. In Proceedings of the 2020 IEEE 7th International Conference on Engineering, 2020.

[9] Salvi, M.; Acharya, U.R.; Molinari, F.; Meiburger, K.M. The Impact of Pre- and Post-Image Processing Techniques on Deep Learning Frameworks: A Comprehensive Review for Digital Pathology Image Analysis. *Comput. Biol. Med.* 2020, 126, 104129.

[10] Khanna, C.; Bish, B.; Kamshetty, D.; Bhardwaj, H.; Bhutani, M. Enhancing License Plate Recognition Using YOLONAS, YOLOv8, and SORT Algorithms. *J. Artif. Intell.* 2025, 2, 167–174.

[11] Ga, K.; P., E.; A., S.; D., V. An Efficient Deep Learning Approach for Automatic License Plate Detection with Novel Feature Extraction. In Proceedings of the 2023 International Conference on Machine Learning and Data Engineering (ICMLDE), Coimbatore, India, 2023.

[12] Omar, N.; Sengur, A.; Al Ali, S.G.S. Cascaded Deep Learning-Based Efficient Approach for License Plate Detection and Recognition. *Expert Syst. Appl.* 2020, 149, 113280.

[13] Delight, D.T.; Velswamy, K. Deep Learning-Based Object Detection Using Mask RCNN. In Proceedings of the 2021 6th International Conference on Communication and Electronics Systems (ICCES), Coimbatore, India, 8–10 July 2021; pp. 948–952.

[14] Alsuwaylimi, A.A. Enhanced YOLOv8-Seg Instance Segmentation for Real-Time Submerged Debris Detection. *IEEE Access* 2024, 12, 1–10.

[15] Lu, M.; Mou, Y.; Chen, C.-L.; Tang, Q. An Efficient Text Detection Model for Street Signs. *Appl. Sci*. 2021, 11, 5962.

[16] Gnanaprakash, V.; Kanthimathi, N.; Saranya, N. Automatic Number Plate Recognition Using Deep Learning. *IOP Conf. Ser. Mater. Sci. Eng*. 2021, 1084, 012027.

[17] Peng, H.; Bayon, J.; Recas, J.; Guijarro, M. Efficient Expiration Date Recognition in Food Packages for Mobile Applications. *Algorithms* 2025, 18, 286

[18] Dewi, C.; Chen, R.-C.; Zhuang, Y.-C.; Manongga, W.E. Image Enhancement Method Utilizing YOLO Models to Recognize Road Markings at Night. *IEEE Access* 2024, 12, 131065–131081.

[19] Fang, S.; Zhang, B.; Hu, J. Improved Mask R-CNN Multi-Target Detection and Segmentation for Autonomous Driving in Complex Scenes. *Sensors* 2023, 23, 3853.

[20] Soni, V.; Shukla, V.; Tandan, S.R.; Pimpalkar, A.; Nema, N.; Naik, M. Performance Evaluation of Efficient and Accurate Text Detection and Recognition in Natural Scenes Images Using EAST and OCR Fusion. *Int. J. Adv. Comput. Sci. Appl.* 2025, 16, 0144.

[21] Talib, M.; Al-Noori, A.; Suad, J. YOLOv8-CAB: Improved YOLOv8 for Real-Time Object Detection. Karbala *Int. J. Mod. Sci.* 2024, 10, 3339.

[22] Li, M., et al. (2021). TrOCR: Transformer-based Optical Character Recognition with Pre-trained Models. Proceedings of the ACM International Conference on Multimedia.

[23] Khalili, B., & Smyth, A. W. (2024). SOD-YOLOv8—Enhancing YOLOv8 for small object detection in aerial imagery and traffic scenes. Sensors, 24(19), 6209.

[24] Khallouli, W., Uddin, M. S., Sousa-Poza, A., Li, J., & Kovacic, S. (2025). Leveraging transformer-based OCR model with generative data augmentation for engineering document recognition. Electronics, 14(1), 5.